Photochemical Synthesis of β-cyclodextrin/Cobalt Oxide Nanoparticles as Photothermal Agents for Photothermal-Induced Enzymatic Reaction

Ludovica Maugeri[∫†], Giuseppe Forte[§†], Maria Anna Messina[∫], Massimo Camarda[♯], Giorgio Ventimiglia[♯], Grazia Maria Letizia Consoli[‡], Salvatore Petralia[§*]

[∫]Expanded Newborn Screening laboratory, A.O.U Policlinico "G. Rodolico San Marco", Via Santa Sofia 78, 95125 Catania, Italy

[§]Department of Drug Science and Health, University of Catania, Viale Andrea Doria 6, 95125 Catania, Italy

[♯]ST-Lab srl, Via Anapo 53, 95126 Catania, Italy

[‡]CNR-Institute of Biomolecular Chemistry, Via P. Gaifami 18, 95126 Catania, Italy

[♯]EM Microelectronic, Rue de Sors 3, 2074 – Marin, Suisse

Supporting Information Placeholder

ABSTRACT: An unprecedent one-pot photochemical method-for the preparation of water-soluble and photothermal nanosized Cobalt$^{(II/III)}$-oxide nanoparticles capped with β-cyclodextrin (β-CD/Co_3O_4) is here reported. This nanomaterial showed the ability to trigger a photothermal-induced enzymatic reaction and in-situ formation of gold nanoparticles. High water solubility and good photothermal conversion efficiency in a wide wavelength range make the β-CD/Co_3O_4 nanoparticles promising candidates for photothermal applications in biomedical field.

Keywords: photothermal effect, nanoparticles, cobalt oxides, cyclodextrin

Photothermal nanostructured materials, due to the ability to convert absorbed light into heat,[1] have received increasing attention for various technological[2] and biomedical applications,[3] including photothermal disease treatment[4] and photothermal-triggered drug release.[5] Cobalt oxides nanoparticles represent an interesting class of photothermal agents, because they possess intense absorbance in the visible and near-infrared regions with good photothermal conversion yield.[6] Their preparation was carried out by using various techniques, including hydrothermal and microwave-assisted methods, and thermal decomposition.[7-9] All these methods need high processing temperature, expensive instrumentation and use of reagents[10]. In contrast the photochemical synthetic approach offers the main advantage to be reagent-free while allowing easy process control, particularly as regards the exposure time and intensity of exciting light. Furthermore, the precursor spectral properties can be used to tune size, morphology, and amount of the resulting nanostructures. In this scenario, thanks to the ability to form adduct and host-guest complexes with metal precursors, β-cyclodextrins (β-CD) were used as microreactors and capping agents for the preparation of stable water-soluble nanoparticles.[11] The modification of the nanoparticle surface by β-CD coating can offer synergistic nanomaterials with novel performances, functions, and applications as photo-responsive nanocomposites[12] and drug delivery systems.[13] Recently, Lu and coworker demonstrated the peroxidase-mimicking performance of cobalt oxide nanoparticles capped with β-CD for the colorimetric determination of ascorbic acid.[14] The ability to induce dual enzymatic and chemical reactions through the photothermal-effect is an appealing and still unexplored application of nanomaterials. The light with its directionality and the nanomaterial site-specific formation permits to induce localized reactions in a specific portion of a surface or solution.

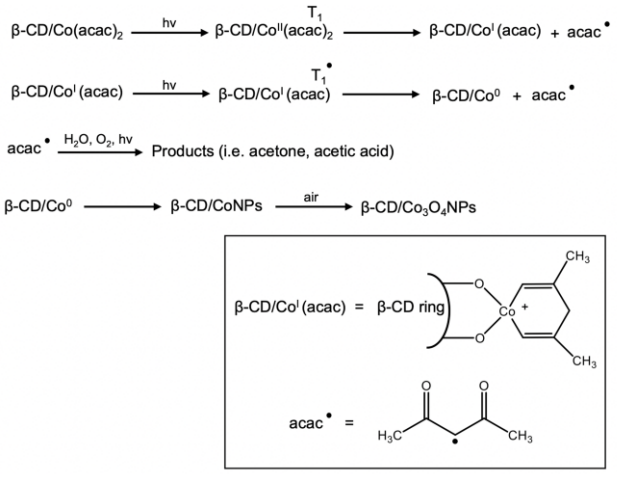

Scheme 1. Photochemical pathway for the β-CD/Co_3O_4 nanoparticles formation. In bracket the structures of the β-CD/Co^I(acac) intermediate and acac• radical species.

Aimed by the above considerations, herein, it is reported an unprecedent one-pot photochemical method for the synthesis of

water soluble Cobalt$^{(II/III)}$ oxide nanoparticles capped with β-CD (β-CD/Co_3O_4) and their potential as photothermal agents for photothermal-induced enzymatic reaction and in-situ formation of gold nanostructures. The water soluble and photothermal β-CD/Co_3O_4 nanoparticles were prepared by photochemical reaction of β-CD-$Co^{II}(acac)_2$ adduct in aerated aqueous solution upon UV light (254 nm) exposition (Scheme 1). Firstly, the interactions between the β-CD and the $Co^{II}(acac)_2$ precursor were widely investigated and demonstrated by UV-Vis spectrophotometry, DLS and Z-potential analysis. Optical absorption spectra showed an increase of the sharp band centered at 291 nm and a broad band centered at 490 nm related to the π→π* intra-ligand absorption and metal-ligand charge-transfer band (LMCT), respectively (SI). The intensity of the bands augmented by increasing the β-CD amount due to the formation of a β-CD-$Co^{II}(acac)_2$ inclusion complex, as recently described by Bai and co-workers.[15] DLS investigations showed that native β-CD in aqueous solution forms self-associated nanoaggregates with a broad distribution hydrodynamic size value of 191 ± 80 nm. As expected, in the presence of $Co(acac)_2$ an increase of the hydrodynamic size value to 368 ± 40 nm suggested the formation of a β-CD/$Co(acac)_2$ adduct.[15] Z-potential analysis indicated that the formation of the β-CD/$Co(acac)_2$ adduct occurs without ligand exchange reaction. Indeed, the Z-potential value for β-CD native nanoaggregates (-21.0 ±2.9 mV) did not drastically change after the β-CD/$Co(acac)_2$ complex formation (-20.0 ± 1.3 mV). Additional data to confirm the β-CD/$Co(acac)_2$ complex formation and in particular the interactions of the Co center with the hydroxyl group of β-CD external ring were obtained by DFT calculation. The electronic energy calculated for the external complex was 21.17 kcal/mol lower than the internal one (SI).

Upon UV irradiation, the acac ligand in β-CD/$Co(acac)_2$ adduct is excited to the triplet state T_1*(π π*), which is involved into the photochemical reactions through a LMCT. The potentials values of the triplet excited state T1* for ketones and enol structures were -1.933 and -2.361 V vs NHE), respectively.[16] Based on these values the T_1* could induce the reduction $Co^{(II)}$ → $Co^{(I)}$ ($E_{redCo(II/I)}$ ~ -0.4V vs SHE). Modelling simulation indicated that the formation of the intermediate β-CD/Co^{I}(acac) species, where the Co-center would be coordinated to one acac and two oxygen atoms of adjacent hydroxyl groups of the β-CD ring, is energetically favorited of 36.47 kcal/mol compared to isolated β-CD and Co^{I}(acac) components.[17-18] Moreover, the calculated absorption spectra highlighted an intense sharp absorption centered at 254 nm and a broad absorption band at 391 nm (Figure 1).

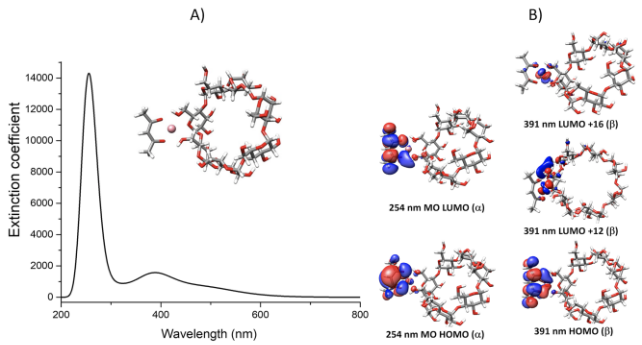

Figure 1. Modelling simulation structure and calculated absorption spectrum for β-CD/Co^{I}(acac).

The analysis of the electronic transitions showed that the main contribution to the band at 254 nm involves the HOMO (α)→LUMO (α) transition (oscillator strength = 0.222). According to the shape of the molecular orbitals (Os) this absorption can be attributed to a π→π* (intra-ligand) transition. While, the lower energy bands (391 nm) consist of two main contributes, HOMO (β) → LUMO +12 (β) and HOMO (β) → L+16 (β) transitions, mainly related to π → d transitions (LMCT) between acac ligand and Cobalt center (Figure 4B). Alle these data indicate that the β-CD/Co_I(acac) can efficiently absorb the excitation light at 254 nm inducing an intra-ligand transition. The excited state T1*(ππ*) of the acac ligand in β-CD/Co^{I}(acac) can induce the reduction of $Co^{(I)}$ to $Co^{(0)}$ resulting in the formation of a metallic cobalt core (β-CD/Co). This plausible pathway was also suggested by the favorable reduction potential value of $Co^{(I)}/Co^{(0)}$ (E_{red} ~ -0.8V vs SHE).[18-19] In aerated condition, the metallic Cobalt core (β-CD/Co) is then oxidized into Co_3O_4 nanoparticles capped with β-CD as indicated by NMR, TEM and HRTEM analyses, while the photogenerated acac• radical species further reacts with O_2 and H_2O to generate side-product as indicated by spectroscopic investigation and as described by Wu et al.[20]

Figures 2A and 2B illustrate the optical absorption spectral changes of β-CD-$Co^{II}(acac)_2$ in aerated and deaerated aqueous solution respectively, upon UV irradiation at different exposure time (0, 5, 10, 15 and 25 min).

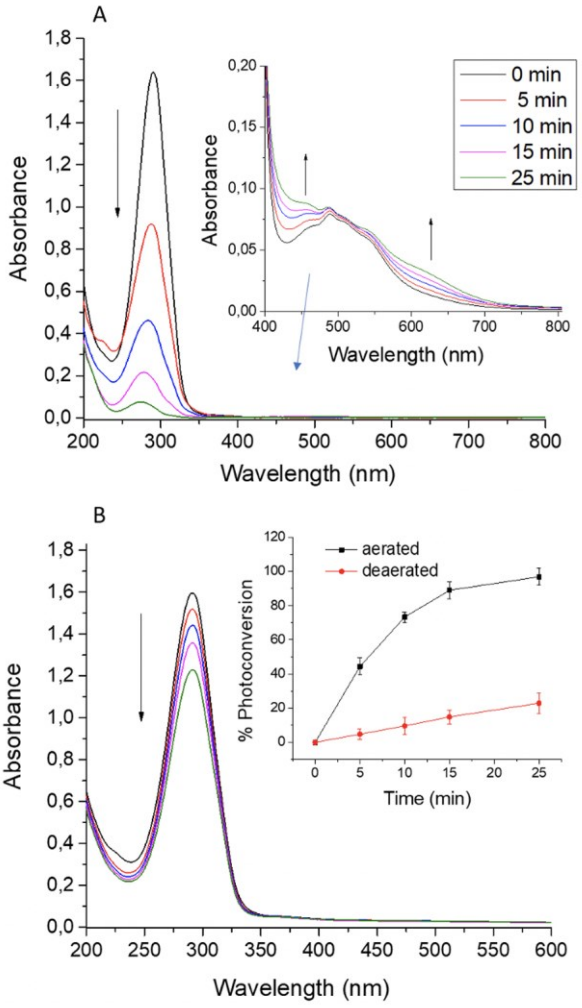

Figure 2. Optical absorption changes of β-CD/$Co(acac)_2$ aqueous solution upon UV-light irradiation in aerated (A) and deaerated (B) conditions. Optical absorption changes in the visible region for the aerated sample (inset A) and photoconversion rate (%) for the aerated and deaerated samples (inset B).

The UV-vis spectra of the aerated samples show a strong decrease of the π→π* intra ligand-band (291 nm), related to the photodegradation of the β-CD-$Co^{II}(acac)_2$ and an increase of the absorbance in the range from 400 to 800 nm (inset Figure 2A) plausibly due to the formation of the β-CD-capped cobalt oxide nanostructures, characterized by a strong absorption in the visible region. Interestingly, the absence of an absorption band below 280 nm suggested that after the photoexcitation the neoformed acac• species is rapidly converted in side-products. The photochemical reaction performed in deaerated condition (Figure 2B) showed a lower photoconversion rate than that obtained in aerated condition. As depicted in the inset in figure 2B, after 25 min of UV exposure, about the 100 % of aerated β-CD-$Co^{II}(acac)_2$ sample was photoconverted into the final products. Contrary, after 25 min only the 25-30 % of deaerated β-CD-$Co^{II}(acac)_2$ was photoconverted. Since the acac• radical species was not rapidly removed, it can promote the reoxidation of $Co^{+} \rightarrow Co^{++}$, resulting in a lower photochemical conversion rate.

The brown-green dispersion obtained by UV light exposure of the β-CD/$Co(acac)_2$ solution in aerated conditions was purified by dialysis in water for 12 hours. The so-obtained green dispersion of β-CD/Co_3O_4 (SI) was fully characterized and tested. Figure 3A shows the optical absorption spectrum of the water dispersed β-CD/Co_3O_4 nanoparticles. The first band in the 300-500 nm range was assigned to the $O^{2-} \rightarrow Co^{2+}$ charge transfer process while the second at higher wavelength (500-900 nm) was consistent with $O^{2-} \rightarrow Co^{3+}$ charge transfer.[21] These two absorption bands indicated the copresence of Co^{2+} and Co^{3+} in the sample, as reported in literature.[22] This data was corroborated by the simulated optical absorption spectra calculated for the β-CD/$Co^{II/III}$ system (SI). The optical band gap energy (E_g) can be determined from the absorption spectra using the equation $(Asshυ)_2 = K (hυ-E_g)$, where Ass is the absorbance coefficient, hυ is the photon energy in eV and E_g is the energy band gap in eV (Figure 3A). Two band gaps for β-CD/Co_3O_4 nanoparticles were estimated, E_{g1}= 2.59 eV (corresponding to valence to conduction band transitions) and E_{g2}= 4.39 eV (corresponding to the $O^{2-} \rightarrow Co^{3+}$ transitions).[22] The E_g values here obtained are greater than those proposed for Co_3O_4 nanostructures by other authors[21,23] due to the smaller size of the β-CD/Co_3O_4 nanoparticles.[24] Figure 3B presents representative cyclic voltammetry curves for β-CD/Co_3O_4 measured in a 0.1 M KOH (scan rate of 10 mV s^{-1}). The analysis revealed two distinct pairs of redox peaks (I and II), with a broad redox background (black line). The redox peaks correspond to the reversible conversion between different cobalt oxidation states. In particular, the first redox peak is ascribed to the redox reaction of Co^{2+}/Co^{3+} and the second redox peak corresponds to the conversion of Co^{3+}/Co^{4+} as widely reported in literature for Co_3O_4 nanostructures[25-28]. As reference the CV analysis for 0.01M β-CD (in 0.1 M KOH scan rate of 10 mV s^{-1}) was performed (red line).
To confirm this data, additionally CV experiments for the precursor $Co(acac)_2$ were performed (0.1 KOH, scan rate 10mV sec^{-1}). The results clearly indicate the presence of a single peak ascribed to the redox reaction of Co^{2+}/Co^{3+} (SI).
The TEM analysis revealed sphere-like nanoparticles (Figure 3C) with mean diameter of 4.9 ± 1.4 nm and narrow size distribution in the range 2-10 nm (SI), surrounded by a carbon nanosized layer, which can be reasonably assigned to the β-CD coating. The lattice resolved HRTEM images, revealed the presence of a crystalline species with d-spacing values of about 2.3 Å and 3.7 Å, attributable to the Co_3O_4 spherical nanoparticles (SI).[24] The presence of Cobalt species in the product β-CD/Co_3O_4 was also confirmed by EDX investigation (SI). The molar ratio of Co and O is 43.8:56.1 (~3:4), within the experimental error, which is consistent with the composition of Co_3O_4. The Z-potential investigations revealed the presence of no-charged β-CD/Co_3O_4 nanostructures, with Z-potential value of + 1.74 ± 3.3 mV. The formation of β-CD/Co_3O_4 nanoparticles was corroborated by ^{1}H-NMR spectra that showed the presence of β-CD signals in the dialyzed sample (Figure 3D). Compared with the typical β-CD proton spectrum, the β-CD proton signals in the cobalt oxide nanoparticles showed a small upfield shift (Δδ 0.013-0.028 ppm range) and broadening consistent with the proximity to the Co_3O_4 core that as a paramagnetic metal center may induce shifts and line-broadening in NMR signals. As a support, no broadening of the β-CD signals was observed when an excess of $Co(acac)_2$ was added to the aqueous solution of β-CD. Moreover, according to the experimental data, computational simulation of the ^{1}H-NMR spectrum showed a small upfield shift for the β-CD signals in the β-CD/Co^{II} nanoparticles (SI).
Photothermal materials with intense light absorption are necessary for high-performing photothermal applications. As shown in Figure 2, the prepared β-CD/Co_3O_4 nanoparticles exhibit large absorption bands for wavelength range from 300 to 900 nm, with absorption intensity high enough to lead to photothermal conversion efficiency into all wavelength range. Thus, three different wavelengths (808, 532 and 405 nm) were chosen to evaluate the photothermal effects of the investigated material. As expected, the β-CD/Co_3O_4 nanoparticles showed good photothermal conversion efficiency (η), with photothermal effect dependent on concentration, wavelength, and laser power (SI). Based on the data recorded, the light-driven photothermal conversion efficiencies were: η_{808nm} = 35.2 %, η_{532nm} = 38.5 % and η_{405nm} = 45.4%, these values are high enough for various photothermal applications[6]. The effective photothermic effect in the 405-808 nm wavelength range, demonstrates the good versatility of the β-CD/Co_3O_4 nanoparticles. According to the conventional photothermal mechanism for semiconductors, upon photothermal excitation, electron–hole pairs are formed with bandgap-like energy (2.59eV). The excited electron finally returns to low-level states by various process including a no-radiative-relaxation that causes the increase of temperature of nanomaterial lattice.

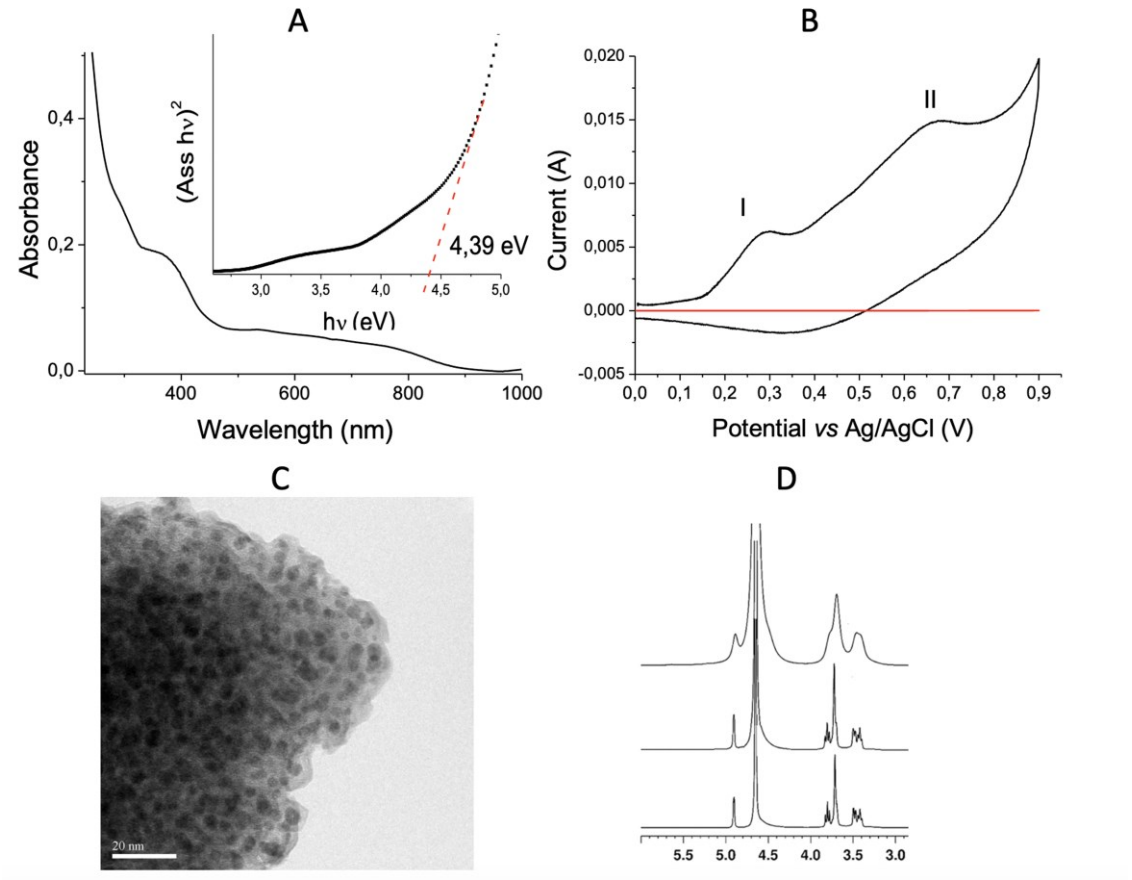

Figure 3. β-CD/Co_3O_4 nanoparticles characterization: A) optical absorption spectra (inset optical band gaps); B) Cyclic voltammogram (CV) curves for β-CD/Co_3O_4 (black line) and 0.01 M β-CD (red line) in 0.1M KOH scan rate 10mV sec^{-1}; C) representative TEM image at 10 K. for β-CD/Co_3O_4; D) ^1H NMR spectra (400 MHz, D_2O, 297 k) in the range 6.0-3.0 ppm of β-CD (5 × 10^{-3} M, bottom), β-CD/$Co(acac)_2$ (5 × 10^{-3} M/7 × 10^{-3} M, middle), and β-CD/Co_3O_4 (top).

To assess the ability of β-CD/Co_3O_4 nanoparticles to promote a photothermal-induced enzymatic reaction, the conversion of phenylalanine to phenylpyruvate, catalyzed by Phenylalanine Dehydrogenase (PDH) in the presence of NAD^+ cofactor, was chosen as reaction model (reaction 1, SI). The produced NADH induced the in-situ formation of gold nanoparticles (reaction 2, SI). The reactions 1 and 2 were performed in the presence of β-CD/Co_3O_4 nanoparticles as photothermal agents. Upon exposure to CW laser (532 nm, power 0.123 W cm^{-2}), the temperature of the sample increased from room temperature (24 ± 1.0 °C) to 37.1 ± 1.5 °C in few minutes (Figure 4A). The photothermal excitation was maintained for 30 min. The occurred reaction 1 was spectroscopically confirmed by the formation of NADH through the typically absorption band centred at 340 nm (Figure 4C). After that, an aliquot of transduction reagent ($AuCl_4^-$/surfactants/seeds) was added to the mixture and the laser power was increased to 0.305 Wcm^{-2}. In this condition the temperature solution increased to a value of 61. ± 1.6 °C (Figure 4A). The photothermal excitation was maintained for 40 minutes. In the reaction 2 the photothermal effect induced the in-situ reduction of $AuCl_4^-$ to Au^0 nanoparticles, spectroscopically detectable by the formation of the typically localized surface plasmon resonance band centred at 543 nm (Figure 4D). The inset in figure 4B shows that the absorbance values at 543 nm increase upon exposure to laser excitation. After about 65 min of light exposition, the temperature of the sample raised-up above 60 °C due to the neo-formed Au^0-nanoparticles, whose absorption at 532 nm promotes an additional photothermal effect (Figure 4A). The so-prepared β-CD/Co_3O_4 nanoparticles did not show mimicking-PDH activity, the main role of these nanostructures was to induce heating of the reaction medium by a photothermal effect, upon green-light excitation. Indeed, no appreciable increase in absorbance at 340 nm (NADH formation) was observed for the experiments conducted in the absence of PHD enzyme. Moreover, the enzymatic NADH formation rate was not influenced by the presence of βCD-Co_3O_4, indeed the same rate was observed when the enzymatic reaction was performed in dark condition (SI) and standard heating with and without nanostructures. This indicated that the βCD-Co_3O_4 do not altered the PHD enzyme acitivity. Moreover, no appreciable increase in absorbance at wavelength values of 340 nm and 534 nm, as well as no increase of temperature were recorded for the black-reference reactions performed radiating an aliquot of sample in the absence of β-CD/Co_3O_4. The main novelty of the of β-CD/Co_3O_4 nanoparticles as photothermal agents for biochemical/chemical reactions are: (i) the high biocompatibility due to the β-CD capping-layer which avoids the enzyme-nanomaterial interactions, that are the main cause of enzyme conformation changes, and (ii) photothermal response in a wide wavelength range, that permits the use of this nanomaterials in a huge of applications. Depending on the application, a limitation could be, the poor stability of the nanomaterial at extreme pH working conditions.

o

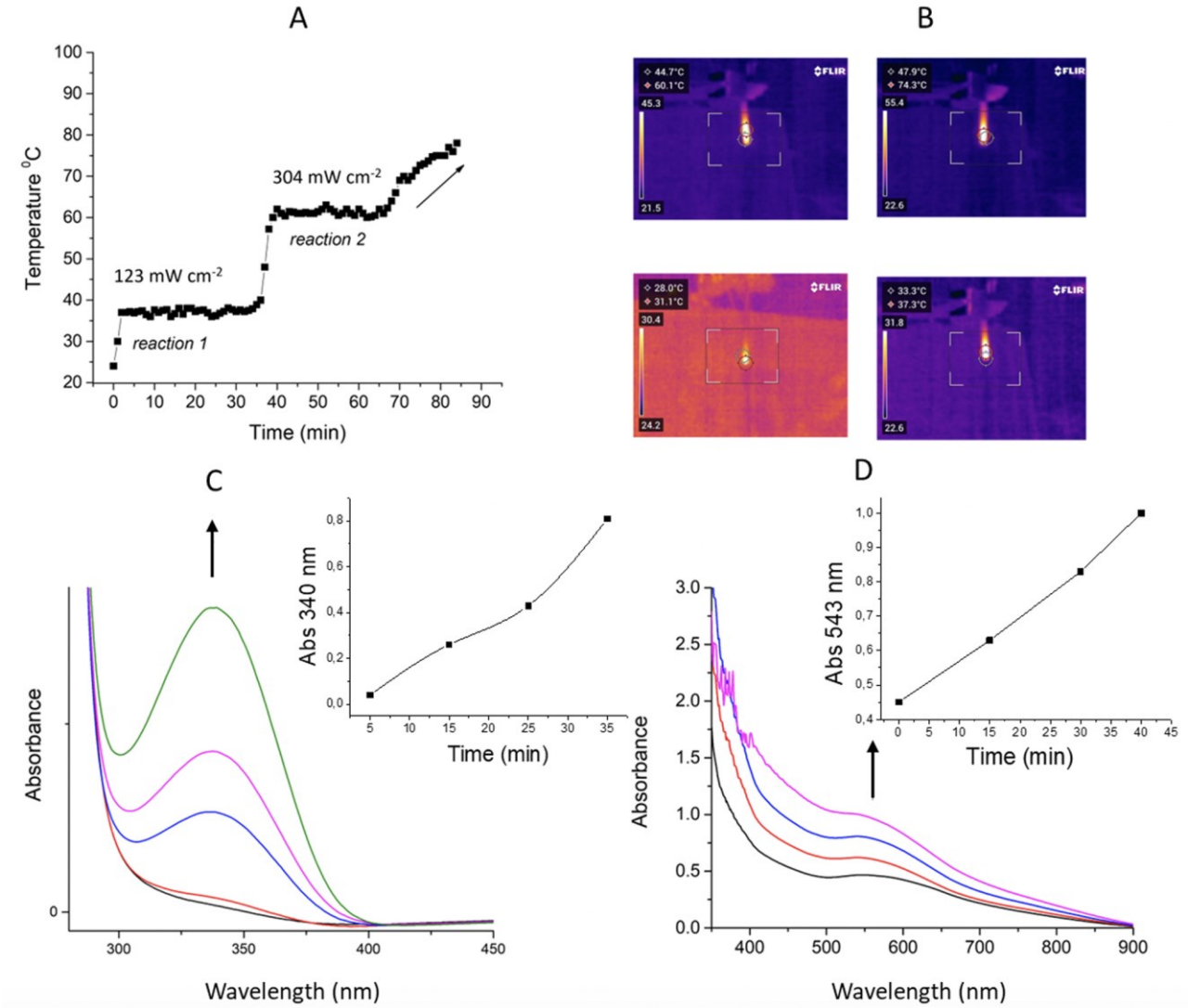

Figure 4. Photothermal-induced enzymatic reaction experiments: A) temperature profile for reaction 1 and 2 upon laser exposure; B) representative thermographs of the mixture during photoexcitation; C) Optical absorption changes for reaction 1, in the inset the increase of the absorption at 340 nm; and D) Optical absorption changes for reaction 2, in the inset the increase of the absorption at 543 nm.

Developing simple and reagent-free new methods to prepare water soluble photothermal nanomaterials is important for future applications in biochemistry and nano-sciences. This work reports a novel, simple, and well-controlled method for the one-pot photochemical synthesis of photothermal β-CD/Co_3O_4 nanoparticles in aqueous solution, without using reducing and photosensitizer agents. UV-photons (254 nm) and air are the only "reagents" used to convert the Co precursor to Cobalt oxides in the presence of β-cyclodextrin as capping agent. This is an advantage compared to the unique example present in literature of β-CD/Co_3O_4 nanoparticles formed from cobalt nitrate and sodium hydroxide endowed with enzyme-mimetic activity. The good photothermal conversion efficiency in a wide wavelength range (405-808 nm), water solubility and nanosize (diameter 4.9 ± 1.4 nm). make the here synthesized nanomaterial appealing for a variety of applications including the photo-induction of enzymatic reactions. Here, we have demonstrated that the β-CD/Co_3O_4 nanoparticles are able to trigger dual photothermal reactions like the enzymatic PHD activity and in-situ gold-nanoparticles formation in aqueous media. Very few examples of photothermal-triggered enzymatic reactions are present in literature, they include activation of lipase by titanium derivate nanosheets[29] and laccase by AuNPs.[30] Therefore, to the best of our knowledges, the here reported nanomaterial is the first example of β-CD/Co_3O_4 nanoparticles synthesized by a photochemical approach and capable to trigger dual photothermal reactions in aqueous medium. These features encourage the use of the β-CD-Co_3O_4 nanoparticles as promising photothermal agents to promote enzymatic reactions in various biosensing applications as photothermal-assisted DNA amplification and photothermal-induces DNA hybridization.

Supporting Information

General information, procedures, analytical data, UV/vis spectra, photothermal data, TEM, EDX data for β-CD-Co_3O_4 nanoparticles (PDF)

Corresponding Author

Salvatore Petralia –
Department of Drug Science and Health, University of Catania, Viale Andrea Doria 6, 95125 Catania, Italy
orcid.org/0000-0001-5692-1130
Email: salvatore.petralia@unict.it.

Author Contributions

† Ludovica Maugeri and Giuseppe Forte equally contributed. The manuscript was written through contributions of all authors. All authors have given approval to the final version of the manuscript.

Notes

The authors declare no competing financial interests.

FUNDING

This research was supported by PKU Smart Sensor" project, funded under Action 1.1.5 POR FESR 2014-2020, CUP G89J18000710007.

REFERENCES

(1) Chen, J.; Ye, Z.; Yang, F.; Yin, Y. Plasmonic Nanostructures for Photothermal Conversion. *Small Sci.* **2021**, *1*, 2000055.

(2) Boldoo, T.; Ham, J.; Kim, E.; Cho, H. Review of the Photothermal Energy Conversion Performance of Nanofluids, Their Applications, and Recent Advances. *Energies* **2020**, *13* (21), 5748.

(3) Qiu, E.; Chen, X.; Yang, D.-P.; Regulacio, M. D.; Ramos, R. M. C. R.; Luo, Z.; Wu, Y.-L.; Lin, M., Li, Z; Loh, X. J.; Ye, E. Fabricating Dual-Functional Plasmonic–Magnetic Au@MgFe2O4 Nanohybrids for Photothermal Therapy and Magnetic Resonance Imaging. *ACS Omega* **2022**, *7*, 2, 2031–2040.

(4) Bian, W.; Wang, Y.; Pan, Z.; Chen, N.; Li, X.; Wong, W.-L.; Liu, X.; He, Y.; Zhang, K.; Lu, Y.-J. Review of Functionalized Nanomaterials for Photothermal Therapy of Cancers. *ACS Appl. Nano Mat.* **2021**, *4*, 11353–11385.

(5) Consoli, G. M. L.; Giuffrida, M. L.; Satriano, C.; Musumeci, T.; Forte, G.; Petralia, S. A novel facile one-pot synthesis of photothermally responsive carbon polymer dots as promising drug nanocarriers. *ChemComm.* **2022**, 58, 3126.

(6) Huang, X.; Cai, H.; Zhou, H.; Li, T.; Jin, H.; Evans, C. E.; Cai, J.; Pi, J. Cobalt oxide nanoparticle-synergized protein degradation and phototherapy for enhanced anticancer therapeutics. *Acta Biomater.* **2021**, *121*, 605–620.

(7) Yetim, N. K. Hydrothermal synthesis of Co_3O_4 with different morphology: Investigation of magnetic and electrochemical properties. *J. Mol. Struct.* 2**021**, *1226*, 129414.

(8) Kumara, R.; Sahoo, S.; Tan, W. K.; Kawamura, G.; Matsuda, A.; .Kar, K. K. Microwave-assisted thin reduced graphene oxide-cobalt oxide nanoparticles as hybrids for electrode materials in supercapacitor, *J. Energy Storage*, **2021**, *40*, 102724.

(9) Gryboś, J.; Hudy, C.; Gryczynska, A.; Piskorz, W.; Sojka, Z. Hydrothermal Synthesis of Euhedral Co_3O_4 Nanocrystals via Nutrient-Assisted Topotactic Transformation of the Layered $Co(OH)_2$ Precursor under Anoxic Conditions: Insights into Intricate Routes Leading to Spinel Phase Development and Shape Perfection. *Cryst. Growth Des.* **2020**, *20* (12), 7771–7787.

(10) Paul, B.; Bhanja, P.; Sharma, S.; Yamauchi, Y.; Alothman, Z. A.; Wang, Z.-L.; Bal, R.; Bhaumik, A. Morphologically controlled cobalt oxide nanoparticles for efficient oxygen evolution reaction. *J. Colloid Interface Sci.,* **2021,** *582*, 322–332.

(11) Petralia, S.; Barbuzzi, T.; Ventimiglia, G. Polymerase chain reaction efficiency improved by water soluble β-cyclodextrins capped platinum nanoparticles. *Mater. Sci. Eng. C*. **2012**, *32*, 848–850.

(12) Ali, S.; Sikdar, S.; Basak, S.; Rajbanshi, B.; Mondal, M.; Roy, D.; Dutta, A.; Kumar, A.; Dakua, V. K.; Chakrabarty, R.; Roy, A.; Barman, A.; Datta, A.; Roy, P. K.; Chakraborty, B.; Roy, M. N. β-Cyclodextrin-Stabilized Biosynthesis Nanozyme for Dual Enzyme Mimicking and Fenton Reaction with a High Potential Anticancer Agent, *ACS Omega* **2022**, *7*, 4457–4470.

(13) Wen, C.; Cheng, R.; Gong, T.; Huang, Y.; Li, D.; Zhao, X.; Yu, B.; Su, D.; Song, Z.; Liang, W. β-Cyclodextrin-cholic acid-hyaluronic acid polymer coated Fe_3O_4-graphene oxide nanohybrids as local chemo-photothermal synergistic agents for enhanced liver tumor therapy, *Colloid. Surfaces B* **2021**, *199*, 111510.

(14) Lu, W.; Zhang, J.; Li, N.; You, Z.; Feng, Z.; Natarajan, V.; Chen, J.; Zhan, V.; Zhan, J.; Lu, W.; Zhang, J. Co3O4@β-cyclodextrin with synergistic peroxidase-mimicking performance as a signal magnification approach for colorimetric determination of ascorbic acid. *Sens. Actuators B Chem*. **2020,** *303*, 127106.

(14) Bai, L; Wyrwalski, F.; Safariamin, M.; Bleta, R.; Lamonier, J.-F.; Przybylski, C.; Monflier, E.; Ponchel, A. Cyclodextrin-cobalt (II) molecule-ion pairs as precursors to active Co_3O_4/ZrO_2 catalysts for the complete oxidation of formaldehyde: Influence of the cobalt source. *J.* Catal. **2016**, *314*, 191–204.

(15) Bai, L.; Wyrwalski, F.; Lamonier, J. F.; Khodakov, A. Y.; Monflier, E.; Ponchel, A. Effects of β-cyclodextrin introduction to zirconia supported-cobalt oxide catalysts: from molecule-ion associations to complete oxidation of formaldehyde. *Appl. Catal. B Environ*. **2013**, *138-139*, 381–390.

(16) Chen, Z.; Song, X.; Zhang, S.; Wu, B.; Zhang, G.; Pan, B. Acetylacetone as an efficient electron shuttle for concerted redox conversion of arsenite and nitrate in the opposite direction. *Water Res*. **2017**, *124*, 331–340.

(17) Lawrence, M. A. W.; Celestine, M. J; Artis, E. T.; Joseph, L. S.; Esquivel, D. L.; Ledbetter, A. J.; Cropek, D. M.; Jarrett, W. L.; Bayse, C. A.; Brewer, M. I.; Holder, A. A. Computational, electrochemical, and spectroscopic studies of two mononuclear cobaloximes: the influence of an axial pyridine and solvent on the redox behaviour and evidence for pyridine coordination to cobalt(I) and cobalt(II) metal centres. *Dalton Trans.* **2016**, *45*, 10326–10342.

(18) Prochowicz, D.; Kornowicz, A.; Lewinski, J. Interactions of native cyclodextrins with metal ions and inorganic nanoparticles: fertile landscape for chemistry and materials science. *Chem. Rev.* **2017**, *117*, 13461–13501.

(19) Rautiainen, A.; Lindblad, M.; Backman, L.; Puurunen, R. L. Preparation of silica-supported cobalt catalysts through chemisorption of cobalt(II) and cobalt(III) acetylacetonate. *Phys. Chem*. *Chem. Phys.* **2002**, *4*, 2466–2472.

(20) Wu, B.; Zhang, G.; Zhang, S. Fate and implication of acetylacetone in photochemical processes for water treatment. *Water Res.* **2016**, *101*, 233–240.

(21) Cheng, S.; Serizawa, M.; Sakata, H.; Hirayama, T. Electrical conductivity of Co_3O_4 films prepared by chemical vapour deposition. *Mater. Chem. Phys*. **1998**, *53*, 225–230.

(22) Bashir, A.; Shukla, S.; Lew, J. H.; Shukla, S.; Bruno, A.; Gupta, D.; Baikie, T.; Patidar, R.; Akhter, Z.; Priyadarshi, A.; Mathews, N.; Mhaisalkar, S. G. Spinel Co_3O_4 nanomaterials for efficient and stable large area carbon-based printed perovskite solar cells. *Nanoscale*, **2018**, *10*, 2341–2350.

(23) Anbika, S.; Gopinath, S.; Saravanan, K.; Sivakuram, K.; Pagupathi, C.; Sukantha, T. A. Structural, morphological and optical properties and solar cell applications of thioglycolic routed nano cobalt oxide material. *Energy Rep.* **2019**, *5*, 305–309.

(24) Gulino, A.; Dapporto, P.; Rossi, P.; Fragalà, I. *Chem. Matter* **2003**, *15*, 2748, 3752 39 Al-Senani, G., M.; Deraz, N. M.; Abd-Elkader, O. H. Magnetic and Characterization Studies of CoO/Co_3O_4 Nanocomposite, *Processes* **2020**, *8*, 844.

(25) Fan, X.; Sun; Y.; Ohlckers, P.; Chen, X. Porous Thin-Wall Hollow Co3O4 Spheres for Supercapacitors with High Rate Capability. *Appl. Sci*. **2019**, *9*, 4672.

(26) Zhou, X.; Shen, X.; Xia, Z.; Zhang, Z.; Li, J.; Ma, Y.; Qu, Y. Hollow Fluffy Co_3O_4 Cages as Efficient Electroactive Materials for Supercapacitors and Oxygen Evolution Reaction. *ACS Appl. Mater. Interfaces* **2015**, *7*, 20322–20331.

(27) Platek, A.; Nita, C.; Ghimbeu, C. M.; Frackowiak, E.-; Fic, K. Electrochemical capacitors operating in aqueous electrolyte with volumetric characteristics improved by sustainable

templating of electrode materials. Electrochim. Acta 2020, 338,135788.
(28) Wang, D.; Wang, Q.; Wang, T. Morphology-Controllable Synthesis of Cobalt Oxalates and Their Conversion to Mesoporous Co_3O_4 Nanostructures for Application in Supercapacitors. *Inorg. Chem.* **2011**, *50*, 6482–6492.
(29) Ding, C.; Liang, J.; Zhou, Z.; Li, Y.; Peng, W.; Zhang, G.; Zhang, F.; Fan, X. Photothermal enhanced enzymatic activity of lipase covalently immobilized on functionalized Ti3C2TX nanosheets, Chem.l Eng. J., **2019**, *378*, 122205.
(30) Guo, S.; Li, H.; Liu, J. Visible-light-induced effects of Au nanoparticle on laccase catalytic activity. *ACS Appl. Mater. Interfaces* **2015**, *7*, 20937–2094.

Graphical abstract